Available online at www.sciencedirect.com

ScienceDirect

Advances in Space Research 71 (2023) 1856–1865

ADVANCES IN SPACE RESEARCH (a COSPAR publication)

www.elsevier.com/locate/asr

Magnetic reconnection on the Sun: ESPD Senior Prize Lecture

Eric Priest

St Andrews University, Mathematics Institute, St Andrews KY16 8QR, UK

Received 31 January 2022; received in revised form 17 March 2022; accepted 23 March 2022
Available online 29 March 2022

Abstract

Magnetic reconnection is a fundamental process for changing the magnetic topology and converting magnetic energy into other forms on the Sun, such as heat, flow energy and fast particle energy. In two dimensions it is fairly well understood, although some aspects still need to be developed. In three dimensions, it behaves very differently and a substantial body of theory and numerical experiment has now been built up, including reconnection at null points, separators and quasi-separators.

Some aspects of solar flares can be understood with 2D reconnection models, but other aspects such as the shapes of flare ribbons, the acceleration of particles and the creation of twist in erupting flux ropes need a 3D understanding. A paradigm shift in our understanding of coronal heating by reconnection has been stimulated by dramatic new observations of photospheric flux cancellation from SUNRISE and from SST together with the realisation that it may well be driving nanoflare heating events and possibly campfires.

Keywords: Magnetohydrodynamics; Magnetic reconnection; ESPD Prize Lecture

1. Introduction

I have been highly fortunate having a career researching such an intriguing and beautiful topic as our Sun. Sharing this journey with such wonderful collaborators has been a real delight, including Jean Heyvaerts, Bernie Roberts, Alan Hood, Peter Cargill, Philippa Browning, Terry Forbes, Pascal Démoulin, Moira Jardine, Mitch Berger, Sami Solanki, Marco Velli, Clare Parnell, Duncan Mackay, Slava Titov, Ineke De Moortel, Gunnar Hornig, Dana Longcope, David Pontin, Fernando Moreno Insertis, Pradeep Chitta, Petros Syntelis and others.

Magnetic reconnection is a fundamental process in a plasma, with three key roles. It changes the magnetic topology, which is turn affects the paths of fast particles and heat, since both travel mainly along the magnetic field. It transfers magnetic energy into heat and bulk kinetic energy, and so tends to produce hot jets of plasma. Finally, in a low-density plasma such as the solar corona, it also converts some of its energy into fast particle energy and so accelerates fast particles by several mechanisms. These include direct electric field acceleration in the reconnection region, shock acceleration especially at termination shock waves that are present where the reconnection jets interact with the surrounding medium, and MHD turbulence created in the reconnection region and the jets.

Here I summarise briefly our latest understanding on the nature of two-dimensional reconnection (Section 2) and and three-dimensional reconnection (Section 3), together with the ways it operates in solar flares (Section 4) and and in chromospheric and coronal heating (Section 5). Detailed arguments and references can be found in two recent reviews (Li et al., 2021; Pontin and Priest, 2022).

2. Two-dimensional reconnection

In two dimensions, magnetic reconnection can take place only at an X-type neutral point in a current sheet.

E-mail address: eric.r.priest@gmail.com

https://doi.org/10.1016/j.asr.2022.03.028
0273-1177/

The basic Sweet-Parker model (Fig. 1) assumes that oppositely directed uniform magnetic fields $\pm B_i$ are carried into a current sheet of length L at uniform speeds $\pm v_i$. This speed is known as the *reconnection rate* and is given in order of magnitude by

$$v_i = \frac{v_{Ai}}{R_{mi}^{1/2}}, \tag{1}$$

in terms of the Alfvén speed ($v_{Ai} = B_i/\sqrt{\mu\rho}$) at the inflow to the sheet and the magnetic Reynolds or Lundquist number

$$R_{mi} = \frac{L v_{Ai}}{\eta}, \tag{2}$$

where η is the magnetic diffusivity.

2.1. Fast spontaneous reconnection

When reconnection is much more rapid than the Sweet-Parker rate, it is known as *fast reconnection*, and there are three ways that fast reconnection may take place in the solar atmosphere. The first is by spontaneous almost-uniform reconnection in a resistive or collisionless medium, when most of the energy is converted at slow-mode MHD shock waves that radiate from a small central current sheet or *diffusion region* (Fig. 2). The phrase "almost-uniform" refers to the fact that the inflow magnetic field lines are only slightly curved away from a uniform field. The reconnection rate (v_e) is then the external inflow speed at large distances (L_e) upstream and is generally quite different from the inflow speed (v_i) at the inflow to the diffusion region.

When the diffusion region is collisional, resistive MHD applies and we have so-called *Petschek reconnection*, when the *local reconnection rate* v_i is given by Eqn. (1) and the global reconnection rate is typically $v_e \approx 0.1 v_{Ae}$ in terms of the external Alfvén speed (v_{Ae}) at large distances (L_e) upstream. However, this applies only when the magnetic diffusivity is enhanced (e.g., by current-driven micro-instabilities), which needs to be demonstrated under solar atmospheric conditions.

On the other hand, when the diffusion region is collisionless, there is currently no theory to model the diffusion region, but local simulations suggest that the local reconnection rate is roughly $v_i \approx (0.01 - 0.1) v_{Ai}$ (e.g., Kleva et al., 1995; Birn et al., 2001), which in turn implies a global reconnection rate of again $v_e \approx 0.1 v_{Ae}$. In this case, there is a need for a global theory to confirm these results.

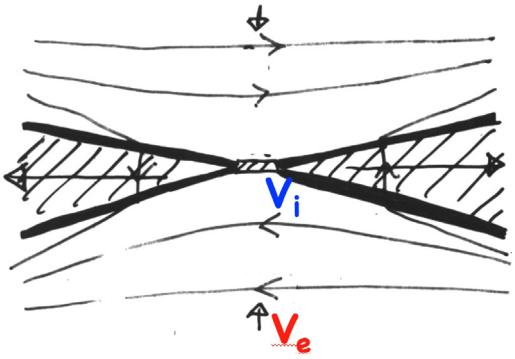

Fig. 2. Fast spontaneous reconnection, in which the thick lines represent slow-mode MHD shock waves.

2.2. Driven reconnection

Rather than being the result of a local instability or resistivity enhancement, reconnection may be driven externally, as in an eruptive solar flare or in a coronal heating event driven by cancelling photospheric flux. In this case, the reconnection will just occur at the driving rate (v_e), up to a maximum allowed rate v_e^*, say. In a steady state, the global rate (v_e) is related to the local rate (v_i) by

$$v_e = v_i \frac{B_i}{B_e}. \tag{3}$$

It depends partly on the local rate and therefore whether the diffusion region is resistive or collisionless, and also on the ratio B_i/B_e and therefore the nature of the ideal inflow region, in particular whether the inflow is converging or diverging (Fig. 3).

When the flow is converging, the maximum rate of reconnection is likely to be $v_e^* \approx 0.1 v_{Ae}$ regardless of whether the diffusion region is resistive or collisionless. However, for a diverging flow the maximum rate is likely to be a multiple of the Sweet-Parker rate ($v_e^* \approx v_{Ae}/R_{me}^{1/2}$) when the diffusion region is resistive, but much faster ($v_e^* \approx 0.1 v_{Ae}$) when it is collisionless.

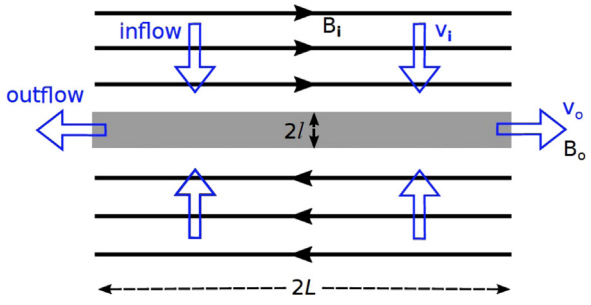

Fig. 1. Sweet-Parker reconnection (from Pontin and Priest (2022) with permission).

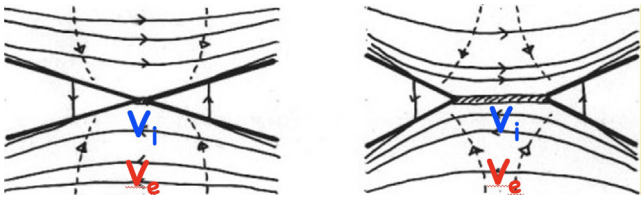

Fig. 3. Driven reconnection for an ideal inflow that is (left) converging or (right) diverging, with thick lines representing slow-mode shocks and flow lines indicated by dashed curves.

2.3. Impulsive bursty plasmoid reconnection

The third scenario that leads to fast reconnection is when the diffusion region becomes so long that it goes unstable to the growth of secondary tearing modes and the reconnection becomes impulsive and bursty (Biskamp, 1982; Forbes and Priest, 1983). Recently, there has been a renewed interest in conducting numerical experiments on this scenario and it has been rechristened *plasmoid instability* (Loureiro et al., 2007; Bhattacharjee et al., 2009) (Fig. 4). These have given a local reconnection rate of $v_i^* \approx 0.01 v_{Ai}$.

As an example, simulations of solar UV bursts driven by emerging or interacting magnetic flux have exhibited impulsive bursty reconnection (Fig. 5).

3. Three-dimensional reconnection

Reconnection in three dimensions is very different from two dimensions in many respects. For example, consider the structure of a null point. In two dimensions, a null forms an X-point or an O-point, but in three dimensions two flux bundles approach a separatrix surface from two sides. Two families of field lines link to the null. The first is an isolated field line called a *spine*, which approaches the null from above and below in Fig. 6, and the second is a surface of field lines called a *fan* which recedes from the null in this example. The fan acts as the *separatrix surface*, which separates the field lines above it from those below it in Fig. 6.

Another difference concerns the topology. In two dimensions, four photospheric sources + - + - in a row in Fig. 7a lead to an X-point in the overlying atmosphere, from which separatrix curves divide the plane up into four distinct 2D regions, in each of which all the field lines join one particular source to another. By contrast, four sources located in a plane that are close enough together produce two three-dimensional null points located in the plane (Fig. 7b). The fan surfaces from these nulls intersect in a special field line, called a *separator*, which joins the nulls. In this case, the fan separatrix surfaces separate the volume into four topologically distinct 3D regions (see Fig. 8).

If the flux sources are spread out or moved below the surface the null points disappear and become regions of low field strength, called *quasi-nulls*, while the separatrices become *quasi-separatrix layers (or QSL's)* and the separator becomes a *quasi-separator*). The region around the quasi-separator is called a *hyperbolic flux tube* (Titov et al., 2002).

In two dimensions, reconnection at the X-point transfers magnetic flux from two regions to the other two regions. The key point, however, about any location where reconnection can take place is that it is a region where the electric current can easily grow to very large values, so that the dif-

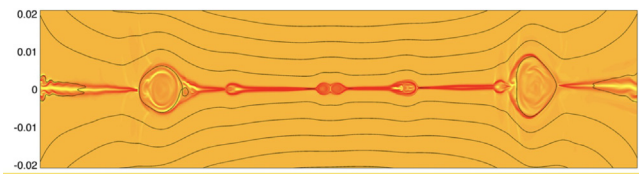

Fig. 4. Plasmoid instability in a long diffusion region (reproduced with permission from Bhattacharjee et al. (2009), copyright by AIP).

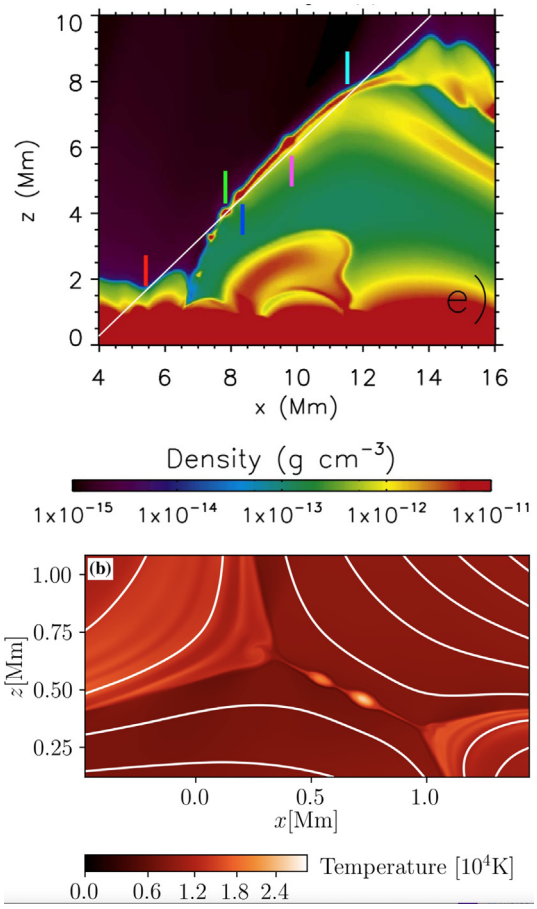

Fig. 5. Examples of plasmoids in simulations of UV bursts in the low solar atmosphere: (above) temperature in a 2D MHD simulation by Peter et al. (2019) of reconnection driven by a photospheric flow; (below) density distribution in a 2.5D radiative MHD simulation by Rouppe van der Voort et al. (2017).

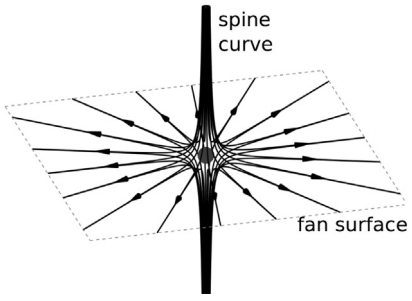

Fig. 6. Structure of a null point in three dimensions, showing the spine field line and fan surface (reproduced with permission from Pontin and Priest (2022), copyright by Springer).

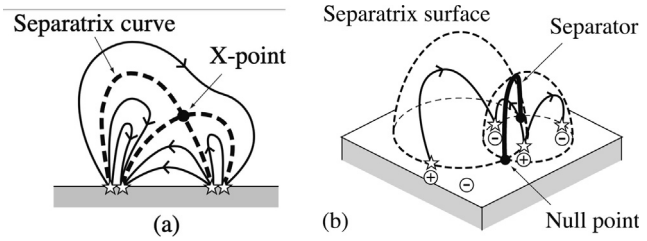

Fig. 7. Magnetic topology due to four flux sources in (a) two dimensions and (b) three dimensions, showing separatrices which intersect in an X-point in 2D and in a separator in 3D. The separatrices are curves in 2D and surfaces in 3D (reproduced with permission from Priest (2014), copyright by CUP).

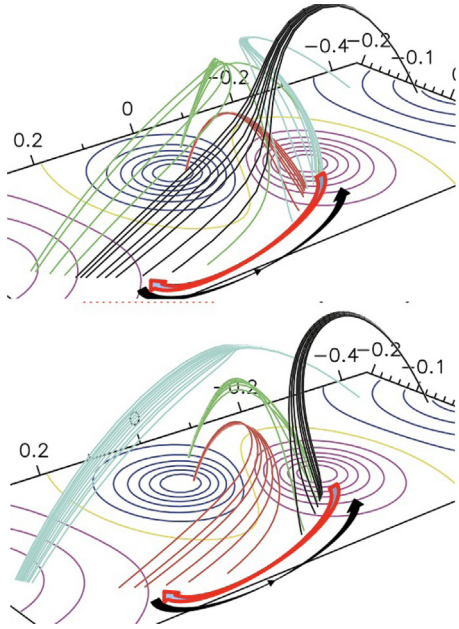

Fig. 8. The flipping of field lines in a numerical simulation of quasi-separator reconnection. Four sets of magnetic field lines are integrated from fixed footpoints and their conjugate footpoints gradually flip along arc-shaped trajectories (reproduced with permission from Aulanier et al. (2006), copyright by Springer).

fusion term in the induction equation can become significant.

In three dimensions, there are four types of magnetic configuration where current tends to accumulate, which produces four types of reconnection, as follows:

* (i) near a null point, especially by so-called *spine-fan reconnection*, when current accumulates at an angle to the spine and fan (Pontin and Galsgaard, 2007; Priest and Pontin, 2009);
* (ii) at a separator by *separator reconnection*, which transfers flux across the separator from two of the 3D regions to the remaining two (Priest and Titov, 1996; Longcope and Cowley, 1996; Galsgaard and Nordlund, 1997; Parnell et al., 2010); in this case there is a discontinuity in the mapping of magnetic field lines from one footpoint to another as the separatrices are crossed;
* (iii) at a quasi-separator by *quasi-separator reconnection* (Priest and Démoulin, 1995; Démoulin et al., 1996a; Titov et al., 2002), when there is a rapid but continuous jump in the footpoint mapping as a quasi-separatrix is crossed;
* (iv) in response to braiding, as first suggested by Parker (1972) and later reviewed in detail by Pontin and Hornig (2020).

In each of these cases, the squashing degree $Q \gg 1$ (Titov et al., 2002; Titov, 2007) and the field lines flip or slip through the plasma (Priest and Forbes, 1992; Pariat et al., 2006; Aulanier et al., 2007; Janvier et al., 2013; Dudík et al., 2014).

4. Solar flares

The usual basic magnetic configuration before an eruptive solar flare is a large-scale twisted flux rope containing an active-region filament or prominence and with overlying magnetic fields that help to keep it anchored down to the solar surface. During the initial stages of such a flare, the flux rope goes unstable or loses equilibrium and begins to rise, stretching out the overlying field lines and probably driving reconnection at a current sheet that forms underneath the flux rope.

Two-dimensional reconnection has been highly successful in accounting for many aspects of solar flares (Fig. 9), such as the formation and heating by reconnection of an arcade of flare loops below the erupting flux rope. It also explains the way new loops are formed at higher and higher altitudes as the reconnection location rises, while old loops cool and form bright separating chromospheric ribbons at their footpoints. As well as being heated by reconnection, the hot flare loops are also very dense since chromospheric plasma at their footpoints is heated by both thermal conduction and fast particles and ablates upwards to fill the

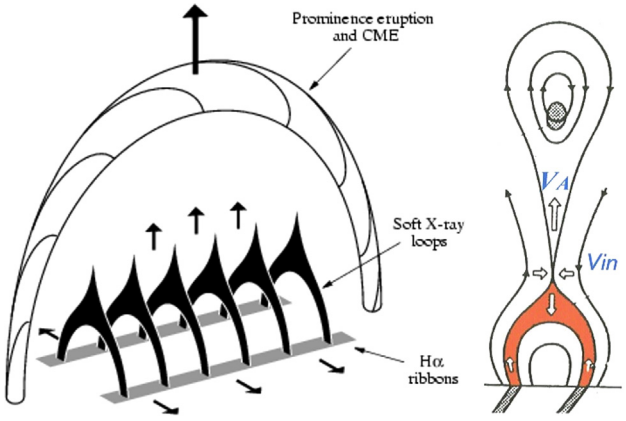

Fig. 9. (Left) A schematic of the overall configuration during an eruptive solar flare, in which rising flare loops with chromospheric ribbons at their feet are created below an erupting flux rope containing a prominence. (Right) A vertical cross-section through the configuration (reproduced with permission from Priest (2014), copyright by CUP).

flare loops. Another feature is that the reconnection adds both magnetic flux and twist to the overlying flux rope.

However, many extra characteristics and effects arise from considerations of 3D reconnection. First of all, some flares occur at a coronal null point by spine-fan reconnection when the null-point fan separatrix forms a dome that arches down to the solar surface and encloses a region of parasitic polarity (Fig. 10). The reconnection then forms a circular chromospheric ribbon where the fan reaches the surface, together with a more remote ribbon where the spine reaches the surface (Masson et al., 2009; Pontin et al., 2013).

Secondly, some flares occur at separators (Longcope and Cowley, 1996; Parnell et al., 2010). For instance, Longcope et al. (2007) have calculated the skeleton of separatrix surfaces for a flaring active region and have explained how the flare spreads through a complex region as separator reconnection occurs at a series of locations that link one subdomain to another (Fig. 11).

Thirdly, other flares occur at quasi-separators with ribbons at the feet of the quasi-separatrix surfaces. The flare energy release and details are very similar to separator reconnection, since the key is that current can build up equally at a separator or a quasi-separator (Mandrini et al., 1997; Aulanier et al., 2006; Pariat et al., 2006; Titov, 2007). This has given rise to the proposal of a standard 3D flare model (Aulanier et al., 2012; Janvier et al., 2014), in which the QSL's or separatrices wrap around the flux rope to produce a sigmoid, whose feet have J-shapes with hook-shaped ends that match the flare ribbons (Fig. 12).

Other three-dimensional effects include the appearance of supra-arcade downflows that are evidence of patchy reconnection (McKenzie and Hudson, 1999; Longcope et al., 2018). Furthermore, in the initial impulsive phase of a flare, bright knots form in the chromosphere and then spread in a direction along the polarity inversion line to form ribbons, which represent the feet of an initial flare loop that expands to form a whole arcade (Fletcher et al., 2004). A model to explain this has been proposed in terms of *zipper reconnection*, which spreads 3D reconnection from one loop to another (Priest and Longcope, 2017). Fig. 13 considers an initial sheared arcad $A_+A_-, B_+B_-, C_+C_-, D_+D_-$, with a weak twisted core Z_+Z_-. It indicates how firstly reconnection of loop A_+A_- with B_+B_- conserving magnetic helicity leads to a loop A_+B_- that is zwisted about Z_+Z_-. Then secondly A_+B_- reconnects with C_+C_- and thirdly with D_+D_- to create a highly twisted core A_+D_-.

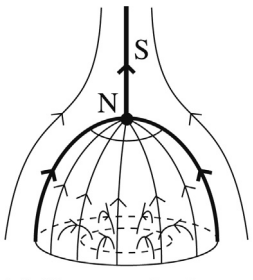

Fig. 10. The topology of a separatrix dome with a coronal null point N lying above a region of parasitic polarity (reproduced with permission from Priest (2014), copyright by CUP).

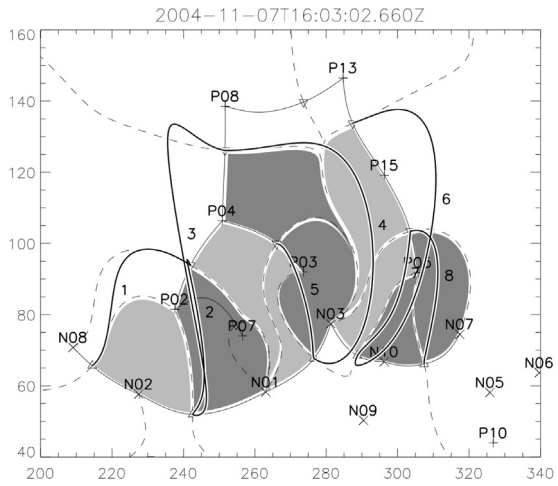

Fig. 11. The skeleton footprint of an active region, showing flux sources, null points, spine curves (solid) and footprints of fan surfaces (dashed), together with separators (thick curves, numbered 1 to 8) and domains that gain (dark) or lose (light) magnetic flux (after Longcope et al., 2007) (reproduced with permission from Priest (2014), copyright by CUP).

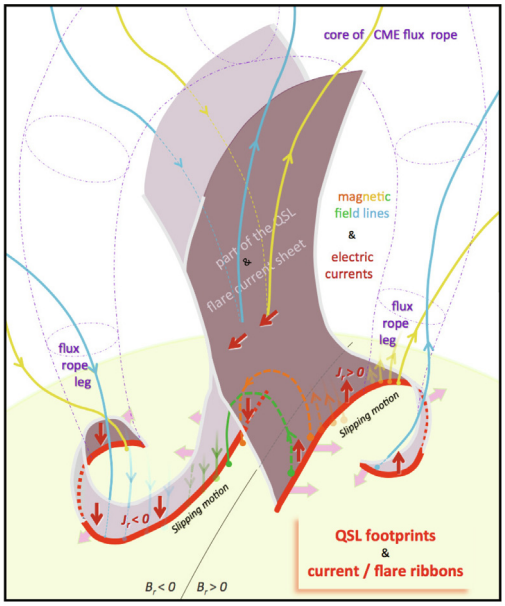

Fig. 12. A cartoon for a 3D model of eruptive flares, showing a QSL (grey) wrapping around an erupting flux rope, together with the outer envelope of the flux rope (blue and yellow) and flare loops that are newly formed by reconnection (green and orange). Image reproduced with permission from Janvier et al. (2014), copyright by AAS.

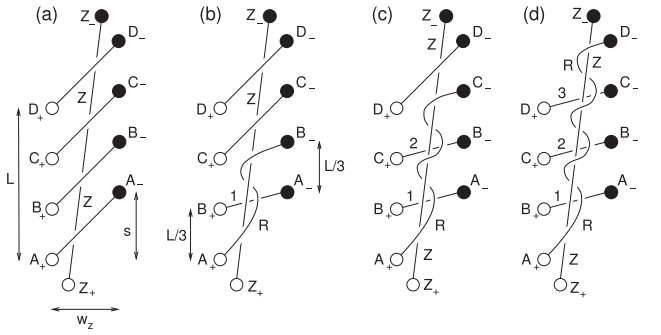

Fig. 13. A zipper model for the creation of flare ribbons and the build-up of twist in an erupting flux rope when the ribbons are observed to form by spreading in one direction from one end of the structure. In other cases, bidirectional spreading of the brightenings is observed in both directions along the polarity inversion line to build up the ribbons, which could be explained by the reconnection starting, not at one end, but some way along the structure and then spreading in both directions away from the starting point. (From Priest and Longcope (2017) with permission.).

4.1. New 3D paradigm for solar flares

A new 3D paradigm has recently been proposed for solar flares (Li et al., 2021; Pontin and Priest, 2022), building on a previous scenario (Aulanier et al., 2012; Janvier et al., 2014) and bringing together a wide range of properties that have been discovered over the past 10 years. Many flares, especially large ones, are eruptive, but in others a strong overlying magnetic field is able to inhibit the eruption and confine the fare. Some flares possess a bipolar magnetic configuration and in others it is multipolar. For multipolar configurations, the basic eruptive process may be similar to that of bipolar configurations but with a more complex field, or the multipolar nature may be crucial to the flare process, as in the breakout model (e.g., Antiochos et al., 1999). If the boundary conditions are assumed to be smooth rather than source-like, the resulting flare process is not greatly affected, since the resulting quasi-separator reconnection is very similar to the separator reconnection that is more common with concentrated flux sources.

In the new 3D paradigm described below, properties (i) and (ii) come from the previous standard 2D paradigm, while most of the others arise from comparisons of flare observations with separator or with quasi-separator reconnection models. Properties (iv), (v), (viii) arise from studies of separators (Longcope and Beveridge, 2007; Titov et al., 2012) and properties (vii), (ix) from quasi-separators (Mandrini et al., 1991; Li et al., 2014; Janvier et al., 2014), but they apply equally to both separator and quasi-separator reconnection.

(i) A magnetic flux rope erupts due to magnetic nonequilibrium or instability (such as torus or kink instability (e.g., Kliem and Török, 2006)) and drives the formation of a current sheet below the flux rope;

(ii) Magnetic field reconnects in the current sheet at a rising location, creating an arcade of rising flare loops with separating chromospheric ribbons at their footpoints;

(iii) Especially late during a flare, at low spatial and temporal resolution, the reconnection may appear quasi-steady and laminar, but, at high resolution, the time-profile is often impulsive and bursty and the energy release is fragmented in space, as evidenced by bright knots of emission during the impulsive phase (Fletcher et al., 2004; Qiu et al., 2017) and supra-arcade downflows during the main phase (McKenzie and Savage, 2009; Longcope et al., 2018);

(iv) Reconnection begins at one location in the current sheet and first energises a single coronal loop with two chromospheric kernels at its feet; during the rise phase, reconnection spreads along the sheet (either unidirectionally from one end or bidirectionally away from a central initial location); this gradually energises the whole coronal arcade and forms the flare ribbons by zipper reconnection (Priest and Longcope, 2017); during the main phase, the arcade of emission rises and the ribbons move apart;

(v) The core of the erupting twisted flux rope may have been present before the eruption, but most of it is created by the 3D reconnection process itself as magnetic shear in the coronal arcade is transferred to twist in the overlying flux rope, while mutual magnetic helicity is converted into self-helicity (van Ballegooijen and Martens, 1989; Wright and Berger, 1989; Priest and Longcope, 2020);

(vi) The most common scenarios are for 3D null-point reconnection to create circular ribbons, or for separator (or quasi-separator) reconnection to create ribbons that are roughly straight or S-shaped; however, other atypical scenarios can arise, such as partially circular ribbons being produced when quasi-separator or separator reconnection occurs above rather than below an erupting structure (Dalmasse et al., 2015);

(vii) The ribbons can possess hook-like ends (Démoulin et al., 1996b; Li et al., 2014), which represent the ends of flux ropes bounded by quasi-separatrix (or separatrix) surfaces (Janvier et al., 2014);

(vii) The structure of highly complex active regions possesses a topology (or quasi-topology) that is split into different domains (or quasi-domains). Reconnection between different domains (or quasi-domains) occurs at separators (or quasi-separators) and allows energy release to spread from one domain (or quasi-domain) to another; the flare ribbons follow a sequence of spines (or quasi-spines) (Longcope and Beveridge, 2007; Kazachenko et al., 2012);

(ix) Flipping or slipping of magnetic fields occurs in all 3D reconnection models and can be observed in the behaviour of flare loops and their footpoints (Mandrini et al., 1991; Dudík et al., 2016).

5. Chromospheric and coronal heating

The evidence seems to be in favour of the high corona being heated by MHD waves of some kind and the low corona and active regions by reconnection in many small current sheets. The initial model for current sheet heating in myriads of nanoflares was by Parker braiding of fields that start out uniform (Parker, 1972), but the coronal tectonics model creates current sheets more easily and takes account of the observational fact that most of the magnetic flux comes through the surface in sources of very small size (Priest et al., 2002). The result is that the flux from each source is separated by separatrix surfaces and QSL's, where current sheets easily form and dissipate in response to photospheric motions (Fig. 14).

A spectacular discovery was made by Chitta et al. (2017) with the SUNRISE balloon mission (Solanki et al., 2010). They observed a region of newly emerging magnetic flux and with Solar Dynamics Observatory (SDO) resolution saw as usual that the feet of coronal loops are unipolar (Fig. 15). However, SUNRISE has a 10 times better spatial resolution for the photospheric magnetic fields and it found instead the presence of mixed polarity magnetic fields at the loop feet. Furthermore, when the mixed polarities cancel, the coronal loops connected to them brighten.

So flux cancellation is much more common than thought previously and is probably important for Ellerman bombs (Rouppe van der Voort et al., 2016; Hansteen et al., 2017), UV bursts (Peter et al., 2014) and also chromospheric and coronal heating.

It suggests that magnetic reconnection near the feet of chromospheric and coronal loops may be heating them, and has formed the basis for a *cancellation nanoflare model* (Priest et al., 2018; Priest and Syntelis, 2021; Chitta et al., 2018; Chitta et al., 2020; Chitta et al., 2021; Peter et al., 2019; Syntelis et al., 2019; Syntelis and Priest, 2020) (Fig. 16). The idea here is that, when two flux sources of opposite polarity approach one another, they drive reconnection in the overlying chromosphere and corona. The length (L) of the reconnecting current sheet and the inflow speed (v_i) and field strength (B_i) at the sheet depend on the size (F) of the flux sources, their speed of approach (v_0) and the overlying field strength (B_0), and these in turn determine the height and amount of the energy release. Indeed, for observed values of the parameters, the heating is found to be sufficient for both the chromosphere and corona. It is therefore a promising candidate to be one of the main contributors to chromospheric and coronal heating.

The original flux cancellation model assumed for simplicity the cancellation of two magnetic fragments of equal strength in an overlying field that is horizontal. It has been extended to include fragments of unequal strength (Syntelis and Priest, 2021) and future extensions may include overlying fields that are inclined or vertical. It is expected that, if the cancellation takes place to the side of the field in the footpoint of an inclined coronal loop, then there will be an asymmetry that is similar to those in Syntelis and Priest (2021). On the other hand, if it takes place within the footpoint, then there will be a coronal null point lying above the minority polarity and so spine-fan reconnection is likely to be driven (Pontin et al., 2013).

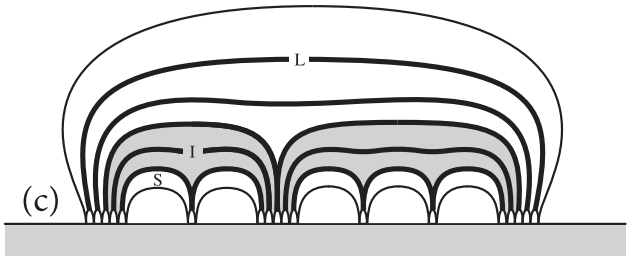

Fig. 14. The tectonics model of chromospheric and coronal heating, showing a schematic of a coronal loop from the side. It possesses many parts, each connecting to a separate flux sources and separated from each other by separatrix surfaces (thick curves). (Reproduced with permission from Priest (2014), copyright by CUP.).

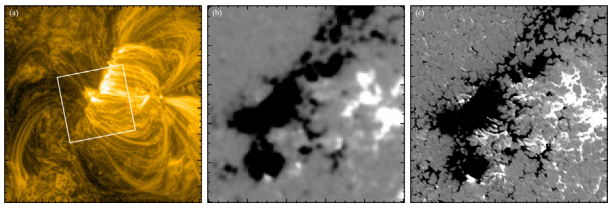

Fig. 15. Coronal image of an active region and the underlying magnetic field. (a) An image from the SDO/Atmospheric Imaging Assembly (AIA) 171 Å filter. (b) SDO/HMI magnetogram showing the distribution of the photospheric line of sight magnetic field for the white box region of panel (a). (c) Same as (b) but for the SUNRISE/IMaX observations. (From Priest et al. (2018) with permission.)

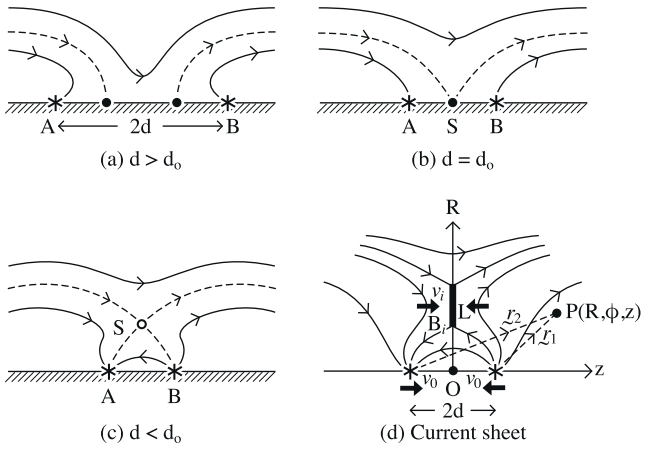

Fig. 16. The flux cancellation model for coronal heating. (a) Two photospheric flux sources ($\pm F$), a distance $2d$ with an overlying field B_0 approach at speed v_0. (b) When $d = d_0$, a separator S is formed, which (c) S which rises as separator reconnection is driven. (d) Magnetic energy is converted at a current sheet of length L. (From Priest and Syntelis (2021) with permission.)

6. Conclusion

Magnetic reconnection has led to many insights into the nature of dynamic phenomena in the solar atmosphere, especially concerning solar flares and atmospheric heating. Major questions about the nature of reconnection that need to be addressed in future have been detailed by Pontin and Priest (2022). As well as understand how it operates in solar flares and coronal heating events, questions include: the ways in which resistivity is enhanced in practice, the nature of the flow in the ideal region around a collisionless or an impulsive bursty current sheet, for driven reconnection the way in which the boundary conditions interact with the diffusion region physics, the nature of spontaneous or driven reconnection when the reconnection is nonuniform. Other major questions include a theory for the coupling of the ideal region with the diffusion region, more details on the nature of 3D reconnection such as its maximum rate and the effect of plasmoid instability, conditions for reconnection onset, effects of partial ionisation and plasma turbulence, and its role in particle acceleration.

Thus, reconnection offers many intriguing questions, whose answers in future will lead to a much deeper understanding from a combination of state-of-the-art theoretical, computational and observational studies. Observations from DKIST and ultra-high resolution space instruments of the vicinity of the reconnection sites will need to be complemented by larger field-of-view measurements over a large temperature range in order to determine the context and consequences of reconnection. For me it has been a real pleasure to play a part in this voyage of discovery which is certain to continue for many years.

Declaration of Competing Interest

The authors declare that they have no known competing financial interests or personal relationships that could have appeared to influence the work reported in this paper.

Acknowledgments

I am delighted to thank my colleagues (listed in the introduction) over the years for all their help and encouragement. It has been a real joy to work with them.

References

Antiochos, S.K., Devore, C.R., Klimchuk, J.A., 1999. A model for solar coronal mass ejections. Astrophys. J. 510, 485–493.

Aulanier, G., Golub, L., DeLuca, E.E., Cirtain, J.W., Kano, R., Lundquist, L.L., Narukage, N., Sakao, T., Weber, M.A., 2007. Slipping magnetic reconnection in coronal loops. Science 318 (5856), 1588. https://doi.org/10.1126/science.1146143.

Aulanier, G., Janvier, M., Schmieder, B., 2012. The standard flare model in three dimensions. I. Strong-to-weak shear transition in post-flare loops. Astron. Astrophys. 543, A110. https://doi.org/10.1051/0004-6361/201219311.

Aulanier, G., Pariat, E., Démoulin, P., Devore, C.R., 2006. Slip-running reconnection in quasi-separatrix layers. Solar Phys. 238, 347–376. https://doi.org/10.1007/s11207-006-0230-2.

Bhattacharjee, A., Huang, Y.M., Yang, H., Rogers, B., 2009. Fast reconnection in high-Lundquist-number plasmas due to the plasmoid instability. Phys. Plasmas 16 (11), 112102.

Birn, J., Drake, J.F., Shay, M.A., Rogers, B.N., Denton, R.E., Hesse, M., Kuznetsova, M., Ma, Z.W., Bhattacharjee, A., Otto, A., Pritchett, P. L., 2001. Geospace environmental modeling GEM magnetic reconnection challenge. J. Geophys. Res. 106, 3715–3720. https://doi.org/10.1029/1999JA900449.

Biskamp, D., 1982. Effect of secondary tearing instability on the coalescence of magnetic islands. Phys. Lett 87A, 357–360. https://doi.org/10.1016/0375-9601(82)90844-1.

Chitta, L.P., Peter, H., Solanki, S.K., 2018. The nature of energy source powering solar coronal loops driven by nanoflares. Astron. Astrophys. 615, 6. https://doi.org/10.1051/0004-6361/201833404.

Chitta, L.P., Peter, H., Solanki, S.K., Barthol, P., Gandorfer, A., Gizon, L., Hirzberger, J., Riethmüller, T.L., van Noort, M., Blanco Rodríguez, J., Del Toro Iniesta, J.C., Orozco Suárez, D., Schmidt, W., Martínez Pillet, V., Knölker, M., 2017. Solar Coronal Loops Associated with Small-scale Mixed Polarity Surface Magnetic Fields. Astrophys. J. Suppl. 229, 4. https://doi.org/10.3847/1538-4365/229/1/4, arXiv:1610.07484.

Chitta, L.P., Peter, H., Young, P.R., 2021. Extreme-ultraviolet bursts and nanoflares in the quiet-Sun transition region and corona. Astron. Astrophys. 647, A159. https://doi.org/10.1051/0004-6361/202039969. arXiv:2102.00730.

Chitta, L.P., Peter, H., Priest, E.R., Solanki, S.K., 2020. Impulsive coronal heating during the interaction of surface magnetic fields in the lower solar atmosphere. Astron. Astrophys. 644, A130. https://doi.org/10.1051/0004-6361/202039099.

Dalmasse, K., Chandra, R., Schmieder, B., Aulanier, G., 2015. Can we explain atypical solar flares? Astron. Astrophys. 574, A37. https://doi.org/10.1051/0004-6361/201323206, arXiv:1410.8194.

Démoulin, P., Henoux, J.C., Priest, E.R., Mandrini, C.H., 1996a. Quasi-separatrix layers in solar flares. I. Method. Astron. Astrophys. 308, 643–655.

Démoulin, P., Priest, E.R., Lonie, D., 1996b. 3D magnetic reconnection without null points. 2. Application to twisted flux tubes. J. Geophys. Res. 101, 7631–7646. https://doi.org/10.1029/95JA03558.

Dudík, J., Janvier, M., Aulanier, G., Del Zanna, G., Karlický, M., Mason, H.E., Schmieder, B., 2014. Slipping magnetic reconnection during an X-class solar flare observed by SDO/AIA. Astrophys. J. 784 (2), 144. https://doi.org/10.1088/0004-637X/784/2/144, arXiv:1401.7529.

Dudík, J., Polito, V., Janvier, M., Mulay, S.M., Karlický, M., Aulanier, G., Del Zanna, G., Dzifčáková, E., Mason, H.E., Schmieder, B., 2016. Slipping Magnetic Reconnection, Chromospheric Evaporation, Implosion, and Precursors in the 2014 September 10 X1.6-Class Solar Flare. Astrophys. J. 823, 41. https://doi.org/10.3847/0004-637X/823/1/41.

Fletcher, L., Pollock, J.A., Potts, H.E., 2004. Tracking of TRACE ultraviolet flare footpoints. Solar Phys. 222, 279–298.

Forbes, T.G., Priest, E.R., 1983. A numerical experiment relevant to line-tied reconnection in two-ribbon flares. Solar Phys. 84, 169–188.

Galsgaard, K., Nordlund, Å., 1997. Heating and activity of the solar corona. III. Dynamics of a low-beta plasma with 3D null points. J. Geophys. Res. 102, 231–248. https://doi.org/10.1029/96JA02680.

Hansteen, V.H., Archontis, V., Pereira, T.M.D., Carlsson, M., Rouppe van der Voort, L., Leenaarts, J., 2017. Bombs and Flares at the Surface and Lower Atmosphere of the Sun. Astrophys. J. 839, 22. https://doi.org/10.3847/1538-4357/aa6844.

Janvier, M., Aulanier, G., Bommier, V., Schmieder, B., Démoulin, P., Pariat, E., 2014. Electric Currents in Flare Ribbons: Observations and Three-dimensional Standard Model. Astrophys. J. 788, 60. https://doi.org/10.1088/0004-637X/788/1/60.

Janvier, M., Aulanier, G., Pariat, E., Démoulin, P., 2013. The standard flare model in three dimensions. III. Slip-running reconnection

properties. Astron. Astrophys. 555, A77. https://doi.org/10.1051/0004-6361/201321164, arXiv:1305.4053.
Kazachenko, M.D., Canfield, R.C., Longcope, D.W., Qiu, J., 2012. Predictions of energy and helicity in four major eruptive solar flares. Solar Phys. 277, 165–183.
Kleva, R.G., Drake, J.F., Waelbroeck, F.L., 1995. Fast reconnection in high temperature plasmas. Phys. Plasmas 2 (1), 23–34. https://doi.org/10.1063/1.871095.
Kliem, B., Török, T., 2006. Torus instability. Phys. Rev. Lett. 96 (25), 255002.
Li, T., Priest, E.R., Guo, R., 2021. Three-dimensional magnetic reconnection in astrophysical plasmas. Proc. R. Soc. A.
Li, Y., Qiu, J., Ding, M.D., 2014. Heating and Dynamics of Two Flare Loop Systems Observed by AIA and EIS. Astrophys. J. 781, 120. https://doi.org/10.1088/0004-637X/781/2/120.
Longcope, D., Beveridge, C., Qiu, J., Ravindra, B., Barnes, G., Dasso, S., 2007. Modeling and Measuring the Flux Reconnected and Ejected by the Two-Ribbon Flare/CME Event on 7 November 2004. Solar Phys. 244, 45–73. https://doi.org/10.1007/s11207-007-0330-7.
Longcope, D., Unverferth, J., Klein, C., McCarthy, M., Priest, E., 2018. Evidence for downflows in the narrow plasma sheet of 2017 september 10 and their significance for flare reconnection. Astrophys J 868 (2), 148, URL: http://stacks.iop.org/0004-637X/868/i=2/a=148.
Longcope, D.W., Beveridge, C., 2007. A quantitative, topological model of reconnection and flux rope formation in a two-ribbon flare. Astrophys. J. 669, 621–635. https://doi.org/10.1086/521521.
Longcope, D.W., Cowley, S.C., 1996. Current sheet formation along three-dimensional magnetic separators. Phys. Plasmas 3, 2885–2897.
Loureiro, N.F., Schekochihin, A.A., Cowley, S.C., 2007. Instability of current sheets and formation of plasmoid chains. Phys. Plasmas 14 (10), 100703.
Mandrini, C.H., Démoulin, P., Bagala, L.G., van Driel-Gesztelyi, L., Henoux, J.C., Schmieder, B., Rovira, M.G., 1997. Evidence of magnetic reconnection from Hα, soft x-ray and photospheric magnetic field observations. Solar Phys. 174, 229–240.
Mandrini, C.H., Démoulin, P., Henoux, J., Machado, M., 1991. Evidence for the interaction of large-scale magnetic structures in solar flares. Astron. Astrophys. 250, 541–547.
Masson, S., Pariat, E., Aulanier, G., Schrijver, C.J., 2009. The nature of flare ribbons in coronal null-point topology. Astrophys. J. 700, 559–578. https://doi.org/10.1088/0004-637X/700/1/559.
McKenzie, D.E., Hudson, H.S., 1999. X-ray observations of motions and structure above a solar flare arcade. Astrophys. J. Letts. 519, L93–L96.
McKenzie, D.E., Savage, S.L., 2009. Quantitative examination of supra-arcade downflows in eruptive solar flares. Astrophys. J. 697, 1569–1577.
Pariat, E., Aulanier, G., Démoulin, P., 2006. A new concept for magnetic reconnection: Slip-running reconnection. In: Barret, D., Casoli, F., Lagache, G., Lecavelier, A., Pagani, L. (Eds.), SF2A-2006: Semaine d'Astrophysique Francaise. Société Francoise d'Astronomie et d'Astrophysique, Paris, pp. 559–562.
Parker, E., 1972. Topological dissipation and the small-scale fields in turbulent gases. Astrophys. J. 174, 499–510. https://doi.org/10.1086/151512.
Parnell, C.E., Haynes, A.L., Galsgaard, K., 2010. The structure of magnetic separators and separator reconnection. J. Geophys. Res. 115, 2102. https://doi.org/10.1029/2009JA014557.
Peter, H., Huang, Y.-M., Chitta, L.P., Young, P.R., 2019. Plasmoid-mediated reconnection in solar uv bursts. Astron. Astrophys. 628, A8. https://doi.org/10.1051/0004-6361/201935820.
Peter, H., Tian, H., Curdt, W., Schmit, D., Innes, D., De Pontieu, B., Lemen, J., Title, A., Boerner, P., Hurlburt, N., Tarbell, T.D., Wuelser, J.P., Martínez-Sykora, J., Kleint, L., Golub, L., McKillop, S., Reeves, K.K., Saar, S., Testa, P., Kankelborg, C., Jaeggli, S., Carlsson, M., Hansteen, V., 2014. Hot explosions in the cool atmosphere of the Sun. Science 346, 1255726. https://doi.org/10.1126/science.1255726, arXiv:1410.5842.
Pontin, D.I., Galsgaard, K., 2007. Current amplification and magnetic reconnection at a three-dimensional null point: Physical characteristics. J. Geophys. Res. 112, A03103. https://doi.org/10.1029/2006JA011848.
Pontin, D.I., Hornig, G., 2020. The Parker problem: Existence of smooth force-free fields and coronal heating. Living Rev. Solar Phys. 17 (1), 5. https://doi.org/10.1007/s41116-020-00026-5.
Pontin, D.I., Priest, E.R., 2022. Magnetic reconnection: Mhd theory and modelling. Living Rev. Solar Phys.
Pontin, D.I., Priest, E.R., Galsgaard, K., 2013. On the nature of reconnection at a solar coronal null point above a separatrix dome. Astrophys. J. 774, 154. https://doi.org/10.1088/0004-637X/774/2/154.
Priest, E., Heyvaerts, J., Title, A., 2002. A Flux Tube Tectonics model for solar coronal heating driven by the magnetic carpet. Astrophys. J. 576, 533–551. https://doi.org/10.1086/341539.
Priest, E.R., 2014. Magnetohydrodynamics of the Sun. Cambridge University Press, Cambridge, UK.
Priest, E.R., Chitta, L.P., Syntelis, P., 2018. A Cancellation Nanoflare Model for Solar Chromospheric and Coronal Heating. Astrophys. J. 862, L24. https://doi.org/10.3847/2041-8213/aad4fc, arXiv:1807.08161.
Priest, E.R., Démoulin, P., 1995. 3D reconnection without null points. J. Geophys. Res. 100, 23443–23463.
Priest, E.R., Forbes, T.G., 1992. Magnetic flipping – reconnection in three dimensions without null points. J. Geophys. Res. 97, 1521–1531. https://doi.org/10.1029/91JA02435.
Priest, E.R., Longcope, D.W., 2017. Flux-Rope Twist in Eruptive Flares and CMEs: Due to Zipper and Main-Phase Reconnection. Solar Phys. 292, 25. https://doi.org/10.1007/s11207-016-1049-0.
Priest, E.R., Longcope, D.W., 2020. The Creation of Twist by Reconnection of Flux Tubes. Solar Phys. 295 (3), 48. https://doi.org/10.1007/s11207-020-01608-0.
Priest, E.R., Pontin, D.I., 2009. Three-dimensional null point reconnection regimes. Phys. Plasmas 16 (12). https://doi.org/10.1063/1.3257901, 122101–122101.
Priest, E.R., Syntelis, P., 2021. Chromospheric and coronal heating and jet acceleration due to reconnection driven by flux cancellation. I. At a three-dimensional current sheet. Astron. Astrophys. 647, A31. https://doi.org/10.1051/0004-6361/202038917. arXiv:2101.04600.
Priest, E.R., Titov, V.S., 1996. Magnetic reconnection at three-dimensional null points. Philos. Trans. R. Soc. A 355, 2951–2992. https://doi.org/10.1098/rsta.1996.0136.
Qiu, J., Longcope, D.W., Cassak, P.A., Priest, E.R., 2017. Elongation of Flare Ribbons. Astrophys. J. 838, 17. https://doi.org/10.3847/1538-4357/aa6341.
Rouppe van der Voort, L., De Pontieu, B., Scharmer, G.B., de la Cruz Rodríguez, J., Martínez-Sykora, J., Nóbrega-Siverio, D., Guo, L.J., Jafarzadeh, S., Pereira, T.M.D., Hansteen, V.H., Carlsson, M., Vissers, G., 2017. Intermittent Reconnection and Plasmoids in UV Bursts in the Low Solar Atmosphere. Astrophys. J. Letts. 851 (1), L6. https://doi.org/10.3847/2041-8213/aa99dd, arXiv:1711.04581.
Rouppe van der Voort, L.H.M., Rutten, R.J., Vissers, G.J.M., 2016. Reconnection brightenings in the quiet solar photosphere. Astron. Astrophys. 592, A100. https://doi.org/10.1051/0004-6361/201628889, arXiv:1606.03675.
Solanki, S.K., Barthol, P., Danilovic, S., Feller, A., Gandorfer, A., Hirzberger, J., Riethmüller, T.L., Schüssler, M., Bonet, J.A., Martínez Pillet, V., del Toro Iniesta, J.C., Domingo, V., Palacios, J., Knölker, M., Bello González, N., Berkefeld, T., Franz, M., Schmidt, W., Title, A.M., 2010. SUNRISE: Instrument, mission, data, and first results. Astrophys. J. Letts. 723, L127–L133. https://doi.org/10.1088/2041-8205/723/2/L127.
Syntelis, P., Priest, E.R., 2020. A Cancellation Nanoflare Model for Solar Chromospheric and Coronal Heating. III. 3D Simulations and Atmospheric Response. Astrophys. J. 891 (1), 52. https://doi.org/10.3847/1538-4357/ab6ffc.
Syntelis, P., Priest, E.R., 2021. Chromospheric and coronal heating and jet acceleration due to reconnection driven by flux cancellation. II. Cancellation of two magnetic polarities of unequal flux. Astron. Astrophys. 649, A101. https://doi.org/10.1051/0004-6361/202140474, arXiv:2103.16184.

Syntelis, P., Priest, E.R., Chitta, L.P., 2019. A Cancellation Nanoflare Model for Solar Chromospheric and Coronal Heating. II. 2D Theory and Simulations. Astrophys. J. 872 (1), 32. https://doi.org/10.3847/1538-4357/aafaf8, arXiv:1901.02798.

Titov, V.S., 2007. Generalized squashing factors for covariant description of magnetic connectivity in the solar corona. Astrophys. J. 660, 863–873. https://doi.org/10.1086/512671.

Titov, V.S., Hornig, G., Démoulin, P., 2002. Theory of magnetic connectivity in the solar corona. J. Geophys. Res. 107, 1164. https://doi.org/10.1029/2001JA000278.

Titov, V.S., Mikic, Z., Török, T., Linker, J.A., Panasenco, O., 2012. 2010 August 1–2 Sympathetic Eruptions. I. Magnetic Topology of the Source-surface Background Field. Astrophys. J. 759, 70. https://doi.org/10.1088/0004-637X/759/1/70.

van Ballegooijen, A.A., Martens, P.C.H., 1989. Formation and eruption of solar prominences. Astrophys. J. 343, 971–984.

Wright, A.N., Berger, M.A., 1989. The effect of reconnection upon the linkage and interior structure of magnetic flux tubes. J. Geophys. Res. 94, 1295. https://doi.org/10.1086/174157.